ARTICLES

Surgeon offsets and dynamic eye movements in laser refractive surgery

Jason Porter, PhD, Geunyoung Yoon, PhD, Scott MacRae, MD, Gang Pan, PhD, Ted Twietmeyer, Ian G. Cox, PhD, David R. Williams, PhD

PURPOSE: To determine the amount of static and dynamic pupil decentrations that occur during laser refractive surgery.

SETTING: The Center of Visual Science and the Department of Ophthalmology, University of Rochester, Rochester, New York, USA.

METHODS: The surgeon's accuracy in aligning the pupil center with the laser center axis was measured when engaging the eye-tracker in 17 eyes receiving conventional laser in situ keratomileusis (LASIK) procedures (Technolas 217z; Bausch & Lomb). Eye movements were measured subsequently during the treatment in 10 eyes using a pupil camera operating at 50 Hz. Temporal power spectra were calculated from the eye movement measurements.

RESULTS: The mean pupil misalignment by the surgeon at the beginning of the procedure was 206.1 μm ± 80.99 (SD) (with respect to the laser center). The laser center was typically misaligned below (inferiorly) and to the left (nasally and temporally in left and right eyes, respectively) of the laser center. Small amounts of cyclotorsion were observed during the ablation (<2 degrees). The mean magnitude of dynamic pupil decentration from the laser center during treatment was 227.0 ± 44.07 μm. The mean standard deviation of eye movements was 65.7 ± 25.64 μm. Temporal power spectra calculated from the horizontal and vertical changes in eye position during the ablation were similar. Ninety-five percent of the total power of the eye movements was contained in temporal frequencies up to 1 Hz, on average, in both directions.

CONCLUSIONS: Most eye movements during LASIK are slow drifts in fixation. An eye-tracker with a 1.4 Hz closed-loop bandwidth could compensate for most eye movements in conventional or customized ablations.

J Cataract Refract Surg 2005; 31:2058–2066 © 2005 ASCRS and ESCRS

Most patients who have conventional or customized laser refractive surgery experience postoperative increases in higher-order aberrations.[1–9] Decentrations of the ablation profile during surgery may account for a portion of these induced aberrations. Ablation offsets result from several factors. Changes in pupil center location from the time aberrations are measured preoperatively over a pharmacologically dilated pupil to the time they are surgically treated over a natural pupil could misalign and statically decenter a customized ablation profile.[10] A static offset of a conventional or customized treatment can also occur when the surgeon manually locks the eye-tracker on the patient's pupil at the beginning or any intermediate stage of the procedure. Errors in the surgeon's visual alignment of the pupil center with the optical axis of the laser system will result in a statically decentered ablation profile and the induction of higher-order aberrations.

Dynamic eye movements and fixation errors by the patient can also influence the actual profile of corneal tissue removed during the treatment. Decentrations caused by eye movements prevent individual pulses from ablating tissue in their intended location. Therefore, the actual ablation profile resulting from these decentrations differs from the originally computed profile, and higher-order aberrations are induced. The use of eye-trackers that measure the eye's position throughout the surgery and provide information used to redirect individual pulses could mitigate the effects of dynamic eye movements on final

0886-3350/05/$-see front matter
doi:10.1016/j.jcrs.2005.08.024

postoperative outcomes.[11] However, a better understanding of the types of eye movements that occur during refractive surgery procedures is needed because these movements largely dictate the requirements of any eye-tracker (such as its closed-loop bandwidth and sampling frequency) used to compensate for changes in eye location.

Two types of eye movements relevant to refractive surgery procedures are torsional and fixational movements. Cyclotorsional eye movements can occur during fixation when the head is laterally tilted from the upright, vertical meridian.[12] Positionally induced cyclotorsion could result in misregistration and rotation of a conventional or customized treatment because aberrations and Phoropter refractions are measured with the patient in an upright position, whereas treatments are performed monocularly with the patient in a supine position. Most findings suggest that cyclotorsional movements between an upright and supine state are not large and would not dramatically affect a refractive surgical procedure.[13–15]

Fixational movements consist of tremor; microsaccades; and large, slow drifts in eye position.[16] Very few publications have reported horizontal and vertical eye movements in fixating patients during laser refractive surgery. In addition, the natural history of eye movements during refractive surgery has not been well documented. Schwiegerling and Snyder[17] recorded eye movements in 5 patients during laser in situ keratomileusis (LASIK) (at a rate of 30 Hz) and found a standard deviation in pupil decentration of approximately 0.10 mm across all eyes. Unfortunately, neither the temporal frequencies nor the speeds of these movements were reported. It is important to monitor fixation stability in patients as they receive their laser refractive surgery treatment. Fixational stability could be worse during LASIK than in normal conditions because LASIK patients are forced to fixate on the center of a light blurred by a cornea that has received a flap cut and is being ablated. This altered surface could increase scatter in the eye and possibly decrease the patient's fixational accuracy. Eye movements influence both the sampling rates and closed-loop bandwidths of an eye-tracker and the amount of higher-order aberrations induced after surgery.

We measured corneal decentrations caused by eye movements in conventional LASIK procedures with an eye-tracker at a frequency equal to the repetition rate of the laser. The surgeon's accuracy in aligning the center of the pupil with the laser system's optical axis when engaging the eye-tracker was determined. We also computed the temporal power spectrum of the measured eye movements to determine the necessary closed-loop bandwidth required of an eye-tracker to compensate for most corneal decentrations in a conventional or customized procedure.

PATIENTS AND METHODS

Seventeen eyes of 9 normal patients were used to determine the surgeon's accuracy in centering the pupil with the laser system's optical axis. The natural history of eye movements was measured during surgery in 10 of these eyes. All patients received conventional LASIK treatments from the same surgeon using the Technolas 217z laser system (Bausch & Lomb) with an active eye-tracker (120 Hz sampling rate). The mean attempted spherical refractive correction was −2.28 diopters (D) ± 1.43 (SD) (range +0.25 to −4.15 D) and the mean attempted cylindrical correction, −0.47 ± 0.45 D.

A pupil camera was inserted into the laser system's optical path to measure eye movements during the LASIK procedures. The camera was placed in a plane conjugate with the cornea and recorded images of the eye that were not altered by any eye-tracker compensation. The frame rate of the pupil camera was electrically synchronized with the repetition rate of the laser (50 Hz) such that an image of the eye was automatically obtained every time a pulse was fired. This method allowed precise determination of the location of the eye each time a laser pulse was delivered to the cornea. The pupil camera first recorded images of the laser's aiming beam when coaligned with the system's optical axis before surgery. Several circular marks were then created on a damp Chayet pad with a pen. The marked pad was placed on the patient's eye after the microkeratome incision was created, where it tightly adhered to the corneal surface and did not move throughout the procedure. These marks were later used to track eye movements during the ablation.

Figure 1 illustrates the pad marks for 1 patient at the first and last frames of the ablation. Any procedure in which the pad moved or was touched by the surgeon was eliminated from the study. It was verified that the pad did not move with respect to fixed features on the eye throughout the treatment. The variability in the distances calculated between these fixed features and the marked spots on the pad during the entire ablation was on the same order or less than the variability in the distances calculated between the

Accepted for publication January 27, 2005.

From the Center for Visual Science (Porter, Pan, Twietmeyer, Williams), University of Rochester, the Department of Ophthalmology (Yoon, MacRae), University of Rochester, and Bausch & Lomb (Cox), Rochester, New York, USA.

Supported by National Institutes of Health grants EY014999, EY01319, EY07125, and EY04367, and research grants from Bausch & Lomb and Research to Prevent Blindness. Also supported in part by the National Science Foundation Science and Technology Center for Adaptive Optics, managed by the University of California at Santa Cruz under cooperative agreement No. AST-9876783.

Drs. Porter, Yoon, MacRae, and Williams have served as consultants to Bausch & Lomb. In addition, the University of Rochester has licensed intellectual property to Bausch & Lomb and has a research contract with them.

Gary Gagarinas, Brenda Houtenbrink, Gina Crowley, Michele Comery, and Joseph Stamm gave technical assistance for the article.

Reprint requests to Jason Porter, PhD, the Center for Visual Science, University of Rochester, Rochester, New York 14627. E-mail: jporter@cvs.rochester.edu.

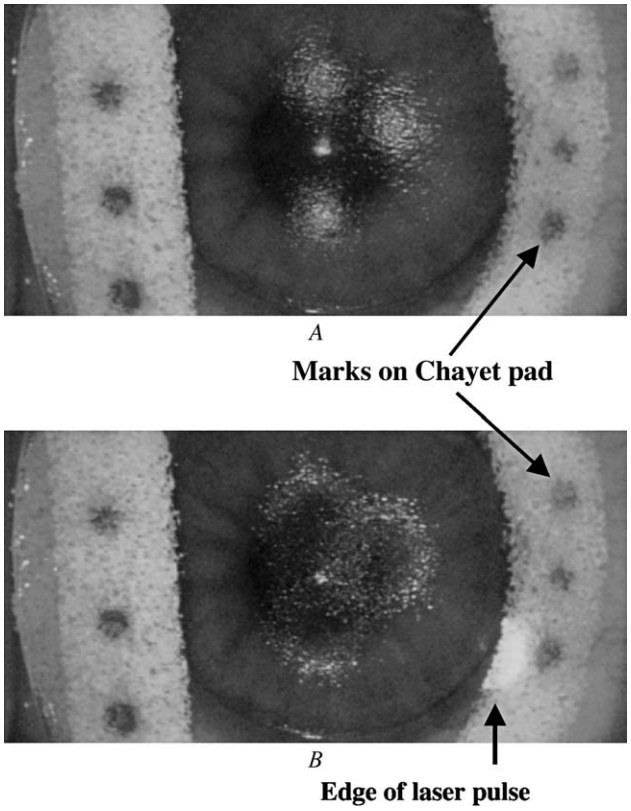

Figure 1. Surgical images of the same eye receiving a conventional LASIK treatment when (*A*) the first pulse was fired and (*B*) the final laser pulse was fired. The pad was marked with spots whose locations were referenced with respect to the center of the pupil from the first frame in *A*. These spots were used to track the eye as it moved during the procedure. A portion of the final laser pulse can be seen in *B* as it strikes the pad.

marked spots alone. This indicates that the movement of the pad on the eye was less than or approximately equal to our accuracy in measuring the movement of the spots on the pad for the entire treatment.

The pupil camera recorded the natural movement of each eye for the entire ablation. The sequence of frames recorded during the treatment was processed after surgery using a custom-written Matlab program (The MathWorks, Inc.) to determine the torsional movements and horizontal and vertical translations for each eye. To determine the surgeon's accuracy in aligning the patient's pupil, the location of the laser system's optical axis was obtained first from the presurgical image of the laser's aiming beam. Each image was analyzed 3 times using the custom-written Matlab program to determine the mean center location of the aiming beam. In this program, a small portion of the image containing the aiming beam was identified manually, and its center coordinates were determined using a center-of-mass algorithm. The repeatability for locating the laser center coordinates, given by the mean across all images of the standard deviations of the 3 measurements, was 4.6 μm (0.18 pixels).

The location of the center of the pupil was determined from the first frame of the procedure (Figure 1, *A*). This pupil image was also analyzed 3 times using the Matlab program. A conventional edge-detection algorithm was used to find the edges of the pupil and a circle was fit to these edges using a nonlinear least-squares technique.[18] The pupil center coordinates were determined from the best-fit circle. The repeatability in determining the pupil center coordinates, given by the mean across eyes of the standard deviations of the 3 measurements within an eye, was approximately 8.2 μm (0.32 pixels). These coordinates were compared with the laser center coordinates to determine the surgeon's accuracy in aligning the patient's pupil with the laser system's optical axis.

When measuring eye movements, it was not possible to track the edge of the pupil for the entire procedure. As shown in Figure 1, the ability to detect the pupil accurately deteriorated as the ablation progressed. The increased scatter observed in Figure 1, *B*, was primarily caused by an increase in corneal surface roughness and a decrease in corneal hydration. Therefore, the pad marks were used to track eye movements during the ablation. First, a box was defined manually around each marked spot in the first recorded frame using our custom program. The centroid location of each spot was determined and then referenced with respect to the pupil center coordinates. Spots that moved outside the image owing to eye movements were not included in the analysis. The Matlab program cross-correlated each spot with its location in the following frame to determine the relative shift of the selected spots between frames. Subpixel accuracy was obtained by determining the center of mass for each spot after the cross correlation with the new frame. A mean horizontal and vertical shift of the eye was computed for each frame based on the shifts of the individual spots. This shift was then added to the previous offset between the pupil and laser center coordinates to determine the new location of the pupil center with respect to the laser system axis for each frame.

The accuracy in determining the horizontal and vertical movements was assessed by examining the variability in the distances calculated between all pairs of marked spots. This analysis was also used to verify whether the pad moved during the treatment. Ideally, if the pad did not move, expand, or contract, the distance between each spot would remain the same across frames. The mean of the standard deviations of all distances between 2 analyzed spots was 7.1 $\pm$ 1.94 μm and ranged between 3.7 and 11.6 μm. This variability in distance was much smaller than a single pixel on the pupil camera (1 pixel $\sim$ 25.5 μm on the eye) and represents the accuracy of the program's ability to detect the center of mass locations of the spots. In procedures in which the pad moved, changes in the distances between spots were considerably larger than these calculated values (ie, typically greater than 51 μm or 2 pixels).

In addition, the rotational movements of each eye during the ablation were measured. To measure cyclotorsion, the custom-written Matlab program constructed a line connecting any 2 of the spots marked on the pad in 1 eye. The program then analyzed the angle made between this line and the horizontal axis (ie, axis = 0 degrees) for each frame in the treatment. (This procedure was replicated for all possible combinations of spots in 1 eye before moving on to repeat the process in the other eyes.) After the angles in each frame were measured, the amount the angles changed for all possible line combinations between consecutive frames were calculated and then the mean of these changes were calculated to obtain a mean amount of rotation between frames. Across all eyes, the mean standard deviations of the cyclotorsional movement was 0.22 $\pm$ 0.08 degrees and ranged between 0.09 degrees and 0.43 degrees. The range of rotation observed during the treatment, calculated as the difference between the maximum and minimum angles subtended by each line, was also determined for

each eye. The mean across all eyes of the range of torsion was 1.22 ± 0.38 degrees and varied between 0.55 degrees and 1.96 degrees. This implies that none of the analyzed eyes experienced torsional movements in excess of 2 degrees.

The amount of astigmatism induced when an astigmatic correction is applied at a fixed rotated angle, A, was calculated. In this case, the eye is rotated to the maximum extent at the very beginning of the procedure and remains in that position for the entire ablation. These calculations represent an upper bound to the amount of astigmatism that can be induced by a fixed torsional movement. The wave aberration for an eye with only astigmatism, $WA_o(\rho,\theta)$, is

$$WA_o(\rho,\theta) = C_2^{-2}\sqrt{6}\rho^2\sin 2\theta + C_2^2\sqrt{6}\rho^2\cos 2\theta \quad (1)$$

where $C_2^{-2}$and C_2^2 are the Zernike coefficients for astigmatism. The wave aberration for astigmatism rotated by A degrees, $WA_r(\rho,\theta)$, is

$$\begin{aligned} WA_r(\rho,\theta) &= C_2^{-2}\sqrt{6}\rho^2\sin[2(\theta+A)] + C_2^2\sqrt{6}\rho^2\cos[2(\theta+A)] \\ WA_r(\rho,\theta) &= \sqrt{6}\rho^2\{[C_2^{-2}\cos 2A - C_2^2\sin 2A]\sin 2\theta \\ &\quad + [C_2^{-2}\sin 2A + C_2^2\cos 2A]\cos 2\theta\} \end{aligned} \quad (2)$$

The residual wave aberration, $WA_R(\rho,\theta)$, after treating the original astigmatic wavefront, $WA_o(\rho,\theta)$, with the rotated astigmatic wavefront, $WA_r(\rho,\theta)$, is

$$\begin{aligned} WA_R(\rho,\theta) &= WA_o(\rho,\theta) - WA_r(\rho,\theta) \\ WA_R(\rho,\theta) &= \sqrt{6}\rho^2\{[C_2^{-2} - C_2^{-2}\cos 2A + C_2^2\sin 2A]\sin 2\theta \\ &\quad + [C_2^2 - C_2^{-2}\sin 2A - C_2^2\cos 2A]\cos 2\theta\} \end{aligned} \quad (3)$$

This expression for the residual wavefront may also be written as

$$WA_R(\rho,\theta) = \sqrt{6}\rho^2\{C_2^{-2^*}\sin 2\theta + C_2^{2^*}\cos 2\theta\} \quad (4)$$

where

$$\begin{aligned} C_2^{-2^*} &= C_2^{-2} - C_2^{-2}\cos 2A + C_2^2\sin 2A \\ C_2^{2^*} &= C_2^2 - C_2^{-2}\sin 2A - C_2^2\cos 2A \end{aligned} \quad (5)$$

$C_2^{-2^*}$and $C_2^{2^*}$are the residual Zernike astigmatism coefficients. For the simple case in which the axis of the patient's cylinder is oriented at 0 degrees or 90 degrees (ie, $C_2^{-2}=0$),

$$C_2^{-2^*} = C_2^2\sin 2A,\ C_2^{2^*} = C_2^2(1-\cos 2A)$$

and the magnitude of residual astigmatism is

$$\sqrt{(C_2^{-2^*})^2 + (C_2^{2^*})^2} = 2|C_2^2||\sin A| \quad (6)$$

Similarly, the magnitude of residual astigmatism when the patient's cylindrical axis is located at 45 degrees or 135 degrees (ie, $C_2^2=0$) is

$$\sqrt{(C_2^{-2^*})^2 + (C_2^{2^*})^2} = 2|C_2^{-2}||\sin A| \quad (7)$$

In these 2 cases, the induced magnitude of astigmatism depends on the initial amount of astigmatism and the sine of the angle of rotation, A.

Figure 2 illustrates the magnitude of astigmatism remaining after an astigmatic correction applied at the minimum, mean, and maximum angles of torsional rotation measured in these eyes as a function of the original amount of astigmatism. The largest attempted cylindrical correction in this group of patients was −1.25 D, and the largest range of torsion was 1.96 degrees. A patient with a cylindrical error of −1.25 D (Zernike astigmatism coefficient ~ 1.15 μm, 6 mm pupil) would theoretically have approximately −0.09 D of cylinder (Zernike astigmatism coefficient ~ 0.079 μm, 6 mm pupil) after an astigmatic correction that was statically rotated by 1.96 degrees. Because this amount of residual astigmatism is small and represents a worst-case scenario for correcting cylinder in our most astigmatic patient, cyclotorsional movements were not included in subsequent calculations.

The temporal power spectra of the horizontal and vertical changes in eye position were calculated to determine the temporal frequency below which most eye movements occurred. The temporal power spectrum succinctly quantifies the size and speed of eye movements that occur at different frequencies. Fast eye movements changing rapidly in time (ie, some saccades) are represented as high temporal frequencies, whereas slow eye movements correspond to lower temporal frequencies. Small amplitude eye movements have low power, whereas eye movements with large amplitudes (or large amounts of movement) have high power.

RESULTS

Pupil and Laser Center Alignment

Figure 3 illustrates the surgeon's accuracy in aligning the center of the patient's pupil with the central laser axis

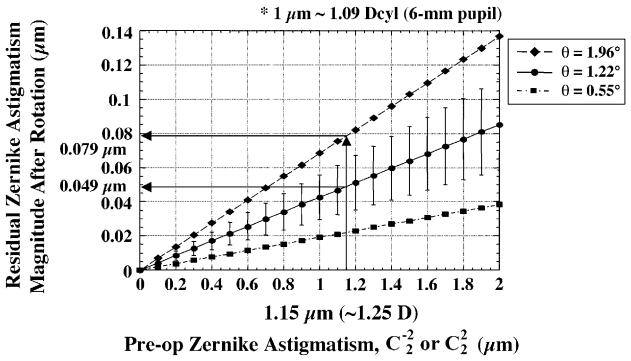

Figure 2. Residual magnitude of astigmatism after applying an astigmatic correction that was rotated by the minimum (0.55 degrees, dashed-dotted line with squares), mean (1.22 degrees, solid line with circles), and maximum (1.96 degrees, dashed line with diamonds) amount of torsional rotation observed in these eyes. The residual astigmatism is plotted as a function of the original (or preoperative) amount of astigmatism for the case when one of the Zernike astigmatism coefficients is equal to zero. For reference, a patient with −1.25 D of cylinder, the maximum value in these eyes would have an original Zernike value of approximately 1.15 μm over a 6.0 mm pupil. After experiencing the maximum amount of torsion (1.96 degrees) for the entire procedure, this patient would theoretically have only −0.09 D of cylinder (0.079 μm of Zernike astigmatism) postoperatively.

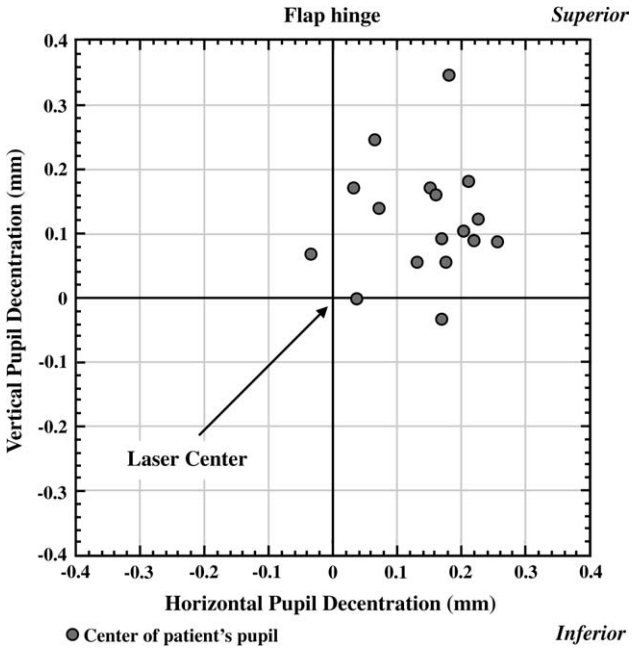

Figure 3. Decentrations in pupil center location in the vertical and horizontal directions when the surgeon best aligned the patient's pupil with the laser center axis. The laser center axis was positioned at the origin of the plot for each eye. Circles indicate the centers of all pupils relative to the laser center axis for 17 eyes at the beginning of the procedure. The superior portion of the eye containing the flap hinge is located at the top of this plot. (Left and right eyes are plotted together.) The pupil was decentered above and to the right of the laser center axis in most eyes, indicating the ablation typically was decentered below (inferiorly) and to the left (nasally and temporally in left and right eyes, respectively) of the patient's pupil center.

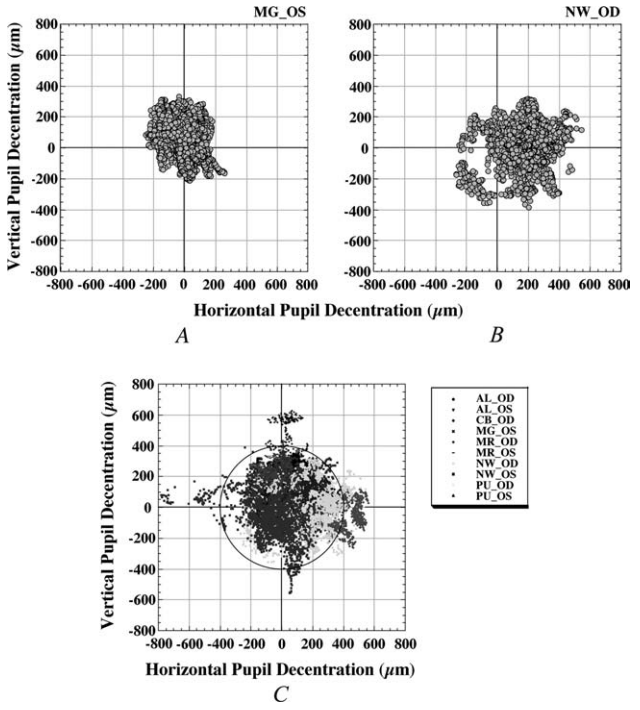

Figure 4. Decentrations in pupil center location for each pulse in (*A*) MG–OS, an eye with little movement about the mean pupil center location, (*B*) NW–OD, an eye with large movements from the mean pupil center location, and (*C*) in all 10 eyes. The central laser axis was positioned at the origin of all plots. Each mark indicates the vertical and horizontal location of the pupil center at an individual pulse relative to the laser center. Nearly all pupil decentrations were confined within a radius of approximately 400 μm (circle) of the laser center.

in 17 eyes. (Left and right eyes are plotted together.) The location of the pupil center relative to the laser center (defined as the origin of the plot) is denoted using a circle for each eye. The mean shift (±SD) in the vertical direction was 122.3 ± 90.28 μm and in the horizontal direction, 141.5 ± 79.99 μm. The mean vector magnitude of the total decentration (calculated as the square root of the sum of the squares of the horizontal and vertical shift in each eye) was 206.1 ± 80.99 μm. In addition, the center of the pupil was consistently decentered above and to the right of the laser center axis in most eyes. This implies that the laser ablation typically was statically offset below (inferiorly) and to the left (nasally and temporally in left and right eyes, respectively) of the patient's pupil center at the beginning of the procedure.

Eye Movements During the Ablation

The changes in the patient's pupil center location relative to the laser center axis during the ablation are shown in Figure 4. The laser center axis was defined as the origin in all plots, and each mark denotes the location of the pupil center relative to the laser center at each laser pulse. The mean horizontal and vertical pupil decentrations from the laser center axis across the 10 measured eyes were 111.8 ± 105.84 μm and 90.1 ± 102.56 μm, respectively, and the mean vector magnitude of pupil decentration from the laser center was 227.0 ± 44.07 μm. There was also high variability in the mean pupil center location across eyes. Some eyes, such as MG–OS (Figure 4, *A*), tended to move about a mean position that was closer to the laser center axis, whereas others, such as NW–OD (Figure 4, *B*), tended to move about a more decentered mean position. Figure 4, C, illustrates the distribution in pupil center location at each pulse in all 10 eyes and shows the amount of movement demonstrated in each eye. As shown in this figure, nearly all of the eye movements were decentered within a vector magnitude of approximately 400 μm from the laser center axis. Table 1 summarizes the mean pupil center locations across all eyes and for eyes MG–OS and NW–OD.

To assess the overall amount of eye movement that occurred during the procedure, the distance between the

Table 1. Mean and range of pupil decentrations from the laser center axis in the horizontal and vertical directions, and the vector magnitude of decentration for all 10 eyes, MG–OS, and NW–OD.

Decentration				
Direction	Magnitude	Mean ± SD (μm)	Minimum (μm)	Maximum (μm)
Horizontal	All 10 eyes	111.8 ± 105.84	−782.4	562.6
	MG–OS	−6.4 ± 101.44	−259.5	254.9
	NW–OD	177.5 ± 143.90	−266.6	541.2
Vertical	All 10 eyes	90.1 ± 102.56	−556.7	625.5
	MG–OS	79.8 ± 116.03	−206.8	336.1
	NW–OD	7.4 ± 132.89	−384.9	316.4
Vector	All 10 eyes	227.0 ± 44.07	0.6	786.9
	MG–OS	158.2 ± 71.52	1.7	353.6
	W–OD	245.3 ± 98.80	8.3	553.5

mean pupil center location and the location of the pupil center at each pulse for the entire procedure was measured in each eye. The standard deviation of the mean distance indicates the variability in pupil center location during the ablation about the mean pupil decentration and indicates the amount of eye movement displayed by the patient. (For example, in an extreme case, an eye with a standard deviation of zero would show no movement about the mean pupil center location. Its pupil center position would remain the same for every pulse, and the eye would be essentially static for the entire ablation.) Some eyes, such as MG–OS (Figure 4, *A*), had small standard deviations resulting from tightly packed distributions in pupil center location relative to the mean pupil location. The small standard deviation indicates that these eyes remained fairly steady about their mean pupil center location during the procedure and exhibited little movement. However, some eyes, such as NW–OD (Figure 4, *B*), had a large standard deviation caused by a broad distribution in pupil center location relative to their mean pupil center location. The large standard deviation in these eyes indicates that they tended to have larger movements in pupil center location throughout the ablation relative to their mean pupil location. The mean standard deviation of the distance between the pupil center location at each pulse and the mean pupil center location across all 10 eyes was 65.7 ± 25.64 μm. Table 2 summarizes the mean of the standard deviation of this distance across the 10 eyes and for MG–OS and NW–OD.

Table 2. Mean and range of the standard deviation of the distance between the pupil center location at each pulse and the mean pupil center location for all 10 eyes, MG–OS, and NW–OD.

Magnitude	Mean Distance ± SD (μm)	Minimum (μm)	Maximum (μm)
All 10 eyes	65.7 ± 25.64	37.3	118.7
MG–OS	56.6	2.0	352.6
NW–OD	98.2	0.8	496.6

Temporal Power Spectra

Temporal power spectra were computed for each eye based on eye movements in the horizontal and vertical directions at a 50 Hz sampling rate during the procedure. The mean power spectra across all 10 eyes in the horizontal and vertical directions are shown in Figure 5, *A*. The percentage of the total power accumulated with increasing temporal frequency for the horizontal and vertical directions were also calculated in each eye. The mean cumulative percentages across all eyes are illustrated in Figure 5, *B*.

The mean temporal power spectra are similar in both directions. As shown in Figure 5, *B*, 95% of the total power of the eye movements was contained in temporal frequencies up to approximately 1.4 Hz in the horizontal direction and approximately 0.6 Hz in the vertical direction. (More than 99% of the total power was accumulated in temporal frequencies up to 5.1 Hz, on average, in both directions.) At a temporal frequency of 1.4 Hz, there was approximately a 380-fold decrease in power, on average, in the vertical and horizontal directions (Figure 5, *A*). These results indicate that most changes in pupil center location during LASIK are caused by relatively slow drifts in eye position.

DISCUSSION

A very important step in properly registering a conventional or customized ablation is to precisely lock the eye-tracker on the center of the patient's pupil. The surgeon must manually align the center of the patient's pupil with the laser center axis and engage the eye-tracker. Inaccuracies in the surgeon's visual alignment of the pupil center with the optical axis of the laser system will result in a statically decentered ablation profile and a subsequent induction of higher-order aberrations. Guirao and coauthors[19] calculated that approximately half the eye's higher-order aberrations would be corrected in a customized ablation that was statically translated by 300 μm or statically rotated by 8 to 10 degrees. The mean vector magnitude of the pupil

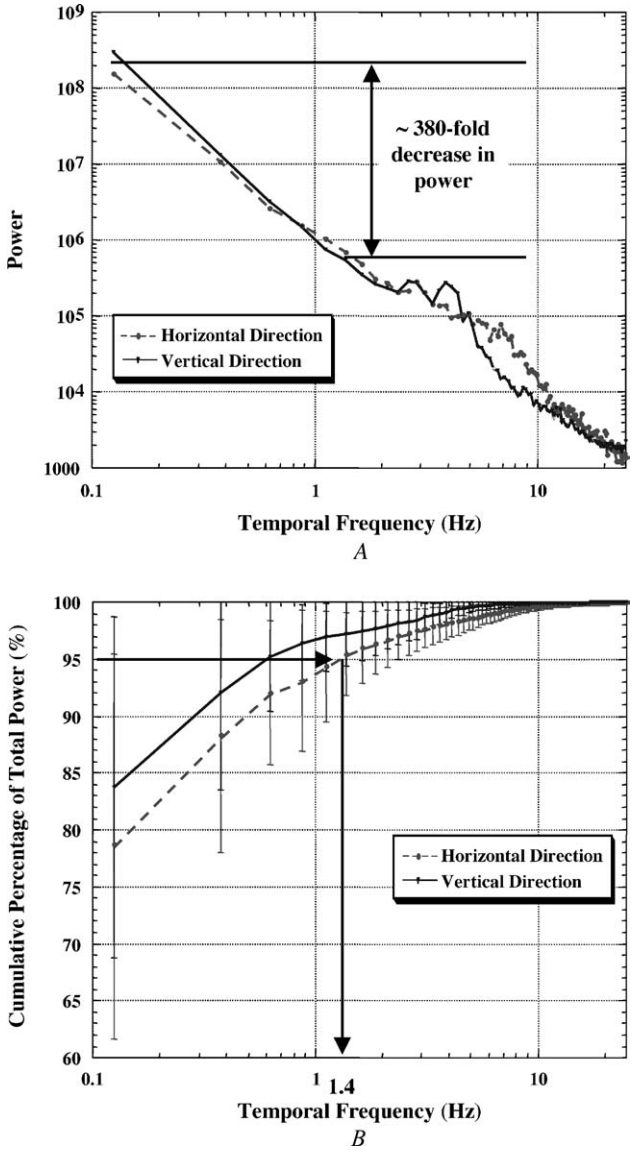

Figure 5. *A*: Temporal power spectra in the horizontal (dashed line) and vertical (solid line) directions averaged across 10 eyes. Eye movements were recorded at a rate of 50 Hz. At a temporal frequency of 1.4 Hz, there was a mean 380-fold decrease in power in both directions. *B*: Average of the cumulative percentage of the total power in the horizontal (dashed line) and vertical (solid line) directions as a function of temporal frequency. Ninety-five percent of the total power was contained in temporal frequencies of up to 1 Hz, on average, in both directions.

decentration from the laser axis owing to the surgeon's visual alignment across 17 eyes was 206.1 ± 80.99 μm. If patients experienced the same amount of decentration in a customized ablation, the treatment would correct approximately 50% of the patient's higher-order aberrations (based on these calculations by Guirao and coauthors). This correction could be even less when including other potential sources of treatment decentrations such as changes in pupil center location between dilated and undilated conditions or dynamic eye movements.

The surgeon consistently decentered the patient's pupil center above and to the right of the laser center axis in most eyes. Therefore, the treatment typically was initially decentered below (inferiorly) and to the left (nasally and temporally in left and right eyes, respectively) of the pupil center in these eyes. Because measurements were recorded over a 2-month span, it is unlikely that the systematic decentration was caused by factors that would affect alignment within a single day, such as a slight misalignment of the surgeon's reticle with the laser axis. The alignment decentrations by the surgeon were consistent and reproducible over time. We do not know whether these decentrations are idiosyncratic to our surgeon or are representative of typical offsets induced by most surgeons during LASIK. Further studies are warranted to resolve this issue.

Cyclotorsional eye movements during fixation can also influence the postoperative aberration structure of the eye. The mean across 10 eyes of the standard deviations of the cyclotorsional movement was 0.22 ± 0.08 degrees and ranged between 0.09 degrees and 0.43 degrees. None of these eyes showed a range in torsional movement larger than 2 degrees. Our observations agree with those in previous reports of the amount of cyclotorsion that occurs during fixation. Carpenter[12] noted that torsional movements are usually less than 7 degrees, but can be as large as 18 degrees. Taylor and Teiwes[13] reported that most cyclotorsional movements in 46 eyes resulted from positional changes. Torsional movements during regular fixation were less than ±1 degree, whereas cyclotorsional movements between the upright and supine condition were larger. Thirty percent of eyes experienced cyclotorsional movements of less than 2 degrees, whereas 70% of eyes had less than 5 degrees of cyclotorsion between the 2 conditions.

Conversely, Smith and Talamo[14] observed cyclotorsions of up to 16 degrees but found no significant difference in cyclotorsion when moving the patient from a seated to supine position in 30 eyes under binocular viewing conditions. Becker and coauthors[15] reported a range of observed cyclotorsion of approximately 2 degrees in 38 eyes and also detected no significant change in cyclotorsion between patients in a seated position under binocular viewing conditions and those in a supine position under monocular conditions. These latter findings indicate that there is no significant difference in cyclotorsional movement between an upright and supine position.[14,15]

We did not include the effects of these small torsional eye movements when calculating pupil decentrations during our conventional treatments because of their relatively

minor impact on postoperative aberrations. The theoretical residual magnitude of astigmatism after applying an astigmatic correction that was rotated at different angles was plotted as a function of the original (or "preoperative") amount of astigmatism in Figure 2. This calculation represented an extreme condition in which the eye maximally rotated at the beginning of the procedure and remained rotated at this angle throughout its duration. The amount of astigmatism remaining after an astigmatic correction of −1.25 D (corresponding to the largest cylindrical refractive error in our 10 eyes) and a static torsional movement of 1.96 degrees (the largest observed range of torsion during fixation) was 0.08 μm (0.09 D over a 6.0 mm pupil). The torsional movements seen in our eyes were also close to the torsional accuracy theoretically required to achieve a diffraction-limited higher-order correction of the eyes' optics. Guirao and coauthors[19] showed their 10 eyes could experience a maximum rotation angle of 3 degrees before their postoperative image quality fell below the Rayleigh limit (ie, Strehl ratio = 0.8) over a 6.0 mm pupil. Bueeler and coauthors[21] calculated that 95% of the 130 eyes required a torsional accuracy of 1 degree or better in a customized procedure to satisfy the Maréchal criteria (ie, rms wavefront error $< \lambda/14$) for a 7.0 mm pupil. The torsional precision was relaxed slightly to 2 degrees or better when correcting only −1.00 D of cylinder and no higher-order aberrations.[20,21]

The range of pupil decentrations from the laser center axis in our 10 measured eyes was similar to that measured in 5 eyes by Schwiegerling and Snyder.[17] The mean horizontal pupil decentration in our eyes was 111.8 ± 105.84 μm and ranged between −39.6 ± 78.20 μm and 275.9 ± 136.59 μm, whereas the horizontal decentrations in Schwiegerling and Snyder's eyes ranged between −45 ± 107 μm and 85 ± 87 μm. Similarly, the mean vertical pupil decentration in our eyes was 90.1 ± 102.56 μm and ranged between −48.3 ± 153.73 μm and 259.3 ± 99.68 μm, whereas the vertical decentrations for Schwiegerling and Snyder's eyes ranged between −19 ± 66 μm and −260 ± 93 μm. Finally, the mean vector magnitude of pupil decentration in our eyes was 227.0 ± 44.07 μm and ranged between 158.2 ± 71.52 μm and 303.0 ± 125.37 μm, whereas the vector magnitude decentrations for Schwiegerling and Snyder's eyes ranged between 200 and 620 μm.

Schwiegerling and Snyder[17] reported a standard deviation in pupil decentration of approximately 100 μm across all eyes. This measure indicates the variance in pupil center location relative to the laser center axis but does not necessarily reflect the true amount of eye movement during the procedure. To obtain a better estimate of the amount of eye movement in our patients during the ablation, we calculated the standard deviation of the mean distance between the mean pupil center location and the location of the pupil center at each pulse for the entire procedure. The mean across all eyes of the standard deviation of these mean distances was 65.7 ± 25.64 μm and ranged between 37.3 μm and 118.7 μm. Eyes with larger standard deviations tended to have larger deviations and movements about their mean pupil center location, indicating less stable fixation.

Temporal power spectra were computed to determine the temporal frequency below which most eye movements occurred. The temporal power spectra calculated from the horizontal and vertical changes in eye position during the ablation were similar. Ninety-five percent of the total power of the eye movements across all 10 eyes was contained in temporal frequencies up to approximately 1 Hz, on average, in both directions (mean values of 1.4 Hz and 0.6 Hz in the horizontal and vertical directions, respectively). More than 99% of the total power was contained in temporal frequencies up to 5.1 Hz, on average, in both directions. Based on these data, we found that the most problematic pupil decentrations during a LASIK procedure result from relatively slow drifts in eye position during fixation. These results agree with earlier findings reported by Yoon et al.[22] and with evidence indicating that observers can use slow eye movements to keep their line of sight locked on a fixation target,[23,24] as patients must do during LASIK. In our cohort of eyes, an eye-tracking system with a 1.4 Hz closed-loop bandwidth could compensate for most pupil decentrations that occur during a conventional or customized laser refractive surgery procedure. In general, an eye-tracker would have to sample at least 10 to 20 times faster than this closed-loop bandwidth, or 15 to 30 Hz, to correct for these movements.

Despite similar spherocylindrical outcomes, early results using an eye-tracker during photorefractive keratectomy and LASIK have shown a significantly smaller increase in 3rd-order aberrations and spherical aberration in eyes treated with an eye-tracker compared with those that did not use an eye-tracker.[11] Nevertheless, there are several areas that can be improved. It will be important to refine techniques to precisely center the patient's pupil with the laser center axis at the beginning or at any intermediate stage of the procedure. A method that can recognize and track a fixed feature or set of features before and during the procedure will reduce the potential for inducing aberrations caused by shifts in pupil center location between dilated and undilated conditions (such as between wavefront measurement and corneal ablation) and any small cyclotorsional errors that may occur. The accuracy and efficiency of the laser ablation also may be improved to become more predictable.[25,26] In addition, we still have much to learn about the biomechanical and healing responses of the post-laser refractive surgery eye. It is also important to

properly instruct the patient about their responsibilities and about what to expect during the procedure.

REFERENCES

1. Oshika T, Klyce SD, Applegate RA, et al. Comparison of corneal wavefront aberrations after photorefractive keratectomy and laser in situ keratomileusis. Am J Ophthalmol 1999; 127:1–7
2. Thibos LN, Hong X. Clinical applications of the Shack-Hartmann aberrometer. Optom Vis Sci 1999; 76:817–825
3. Williams DR, Yoon GY, Porter J, et al. Visual benefit of correcting higher order aberrations of the eye. J Refract Surg 2000; 16:S554–S559
4. Mrochen M, Kaemmerer M, Seiler T. Clinical results of wavefront-guided laser in situ keratomileusis 3 months after surgery. J Cataract Refract Surg 2001; 27:201–207
5. Mrochen M, Kaemerrer M, Mierdel P, Seiler T. Increased higher-order optical aberrations after laser refractive surgery: a problem of subclinical decentration. J Cataract Refract Surg 2001; 27:362–369
6. Endl MJ, Martinez CE, Klyce SD, et al. Effect of larger ablation zone and transition zone on corneal optical aberrations after photorefractive keratectomy. Arch Ophthalmol 2001; 119:1159–1164
7. Moreno-Barriuso E, Lloves JM, Marcos S, et al. Ocular aberrations before and after myopic corneal refractive surgery: LASIK-induced changes measured with laser ray tracing. Invest Ophthalmol Vis Sci 2001; 42:1396–1403
8. Marcos S, Barbero S, Llorente L, Merayo-Lloves J. Optical response to LASIK surgery for myopia from total and corneal aberration measurements. Invest Ophthalmol Vis Sci 2001; 42:3349–3356
9. Aizawa D, Shimizu K, Komatsu M, et al. Clinical outcomes of wavefront-guided laser in situ keratomileusis: 6-month follow-up. J Cataract Refract Surg 2003; 29:1507–1513
10. Porter J, Yoon G, Lozano D, et al. Aberrations induced in customized laser refractive surgery due to shifts between natural and dilated pupil center locations. In press, J Cataract Refract Surg
11. Mrochen M, Salah Eldine M, Maemmerer M, et al. Improvement in photorefractive corneal laser surgery results using an active eye-tracker system. J Cataract Refract Surg 2001; 27:1000–1006
12. Carpenter RHS. Movements of the Eyes. London, Pion Limited, 1988
13. Taylor N, Teiwes W. Eye tracking and alignment in refractive surgery: requirements for customized ablation. In: Krueger R, Applegate RA, MacRae S, eds, Wavefront Customized Visual Correction: The Quest for SuperVision II. Thorofare, NJ, Slack, 2004; 195–202
14. Smith EM, Talamo JH. Cyclotorsion in the seated and supine patient. J Cataract Refract Surg 1995; 21:402–403
15. Becker R, Krzizok TH, Wassill H. Use of preoperative assessment of positionally induced cyclotorsion: a video-oculographic study. Br J Ophthalmol 2004; 88:417–421
16. Ditchburn RW, Foley-Fisher JA. Assembled data on eye movements. Optica Acta 1967; 14:113–118
17. Schwiegerling J, Snyder RW. Eye movements during laser in situ keratomileusis. J Cataract Refract Surg 2000; 26:345–351
18. Press WH, Teukolsky SA, Vetterling WT, Flannery BP. Numerical Recipes in C: The Art of Scientific Computing, 2d ed. New York, NY, Cambridge University Press, 1997
19. Guirao A, Williams DR, Cox IG. Effect of rotation and translation on the expected benefit of an ideal method to correct the eye's higher-order aberrations. J Opt Soc Am 2001; 18:1003–1015
20. Williams DR, Porter J, Yoon GY, et al. How far can we extend the limits of human vision? In: Krueger R, Applegate RA, MacRae S, eds, Wavefront Customized Visual Correction: The Quest for SuperVision II. Thorofare, NJ, Slack, 2004; 17–38
21. Bueeler M, Mrochen M, Seiler T. Maximum permissible torsional misalignment in aberration-sensing and wavefront-guided corneal ablation. J Cataract Refract Surg 2004; 20:17–25
22. Yoon GY, Kwon C, MacRae S, et al. Effect of corneal decentration on the outcome of laser refractive surgery procedure. 3rd International Congress of Wavefront Sensing and Aberration-Free Refractive Correction 2002 (Interlaken, Switzerland)
23. Steinman RM, Cunitz RJ, Timberlake GT, Herman M. Voluntary control of microsaccades during maintained monocular fixation. Science 1967; 155:1577–1579
24. Steinman RM, Haddad GM, Skavenski AA, Wyman D. Miniature eye movement. Science 1973; 181:810–819
25. Mrochen M, Seiler T. Influence of corneal curvature on calculation of ablation patterns used in photorefractive laser surgery. J Refract Surg 2001; 17:S584–S587
26. Yoon G, MacRae S, Williams DR, Cox IG. Causes of spherical aberration induced by laser refractive surgery. J Cataract Refract Surg 2005; 31: 127–135